

Operation of the induction motor supplied with a distorted voltage

Tomasz Drabek^{a,*}, Krzysztof Krzyściak^{*}

^a AGH University of Science and Technology, al. Mickiewicza 30, 30-059 Krakow, Poland

^b University of Applied Sciences in Tarnow, ul. Mickiewicza 8, 33-100 Tarnow, Poland

Article history:

Received 13 March 2020

Received in revised form

28 April 2020

Accepted 29 April 2020

Available online 6 May 2020

Abstract

The paper presents the theoretical basis of the mathematical expression derived from the American standard, used to determine the thermally permissible torque load capacity of the cage induction motors when supplied with distorted voltages. The results of the measurement verification of this expression for different voltage shapes supplying the tested motor are presented. The test results confirmed the correctness of the expression when the motor is supplied with distorted voltage with a limited number of higher harmonics.

Keywords: Induction motor, distorted power supply, HVF factor, load capacity

Introduction

Powering an induction motor with a three-phase voltage containing additional harmonic frequencies in relation to the fundamental frequency of 50 Hz ($f_h = 100, 150, 200, 250, 300 \dots$ Hz) can be a source of many disturbances in its operation, and above all, it causes an increase in power losses in the motor and generation of alternating torques [1, 2, 3]. This causes the necessity to lower the thermally permissible motor load capacity in terms of torque and power. The source work [4] presents considerations leading to the determination of the permissible load capacity of a cage induction motor supplied with distorted voltage, depending on the size of this distortion. The expression derived there is now commonly used. This expression was derived with the following assumptions:

1. It is limited to the first rotating harmonics (with the numbers $h = 5, 7, 11, 13, 17, 19$), omitting the third harmonics ($h = 3, 9, 15, \dots$) and even harmonics ($h = 2, 4, 6, \dots$) as well as interharmonics and subharmonics. The full symmetry of distorted voltages was assumed. Harmonics of voltages: 5, 11, 17 give magnetic fields in the machine, which rotate in the opposite direction to the rotor rotation, and harmonics 7, 13, 19 – fields that rotate in the direction of rotor rotation.
2. Classic equivalent circuits of a ring induction machine for the above-mentioned harmonics were used [5, 6]. However, the rotor slip in relation to all the considered higher harmonics was ignored, assuming slip equal to 1, on the basis of large differences between the speeds of the higher harmonics magnetic field and the subsynchronous rotor speed.

3. In each of the equivalent electric schemes for individual harmonics, its magnetizing branch was omitted, and only the load losses were considered for the calculation of thermal load of the machine. However, the idle losses were taken into account indirectly, by their presence in the total power losses of the machine in the rated condition.
4. The short-circuit reactance of the equivalent circuit for each harmonic was assumed in the form:

$$X_{khr} = (X_{\sigma s1} + X_{\sigma r1}') \cdot h^{0.8} = X_{k1r} \cdot h^{0.8} \quad (1)$$

Where: $X_{\sigma s1}$ is the stator leakage reactance for the first harmonic ($h = 1$), i.e. for the rated frequency (in [4] for 60Hz), $X_{\sigma r1}'$ – start-up value (for $s = 1$) of the rotor leakage reactance for the first harmonic.

The stator leakage inductance $L_{\sigma s1}$ was assumed to be absolutely constant ($L_{\sigma sh} = L_{\sigma s1}$), in contrast to the rotor leakage inductance, decreasing with increasing slip and with increasing supply frequency. This variability has been included in the expression (1).

5. The short-circuit resistance of the equivalent circuit for each harmonic was assumed in the form:

$$R_{khh} = (R_s + R_{r1}' + R_{d1}) \cdot h^{0.6} = R_{k1} \cdot h^{0.6} \quad (2)$$

where: R_s is the stator phase resistance; R_{r1}' is the rotor resistance value for the first harmonic and normal motor operating slips (a several percent), and R_{d1} is the resistance representing additional losses in the machine for the first harmonic. The stator phase resistance was assumed to be absolutely constant and equal to the resistance measured with direct current, in contrast to the rotor resistance, which increases with increasing slip and with increasing frequency of the supply. The resistance R_d was assumed as increas-

*Corresponding author:

drabek@agh.edu.pl, krzysztof.krzyściak@adres.pl

ing with the harmonic number according to the formula:

$$R_d = R_{d1} \cdot h^{0.8} \quad (3)$$

The variability of the values of the resistance R_{rl} and R_{dl} were taken into account in the expression (2).

6. For higher harmonics ($h \geq 5$) the relationship is: $X_{khr} \gg R_{kh}$.

On this basis, it was assumed that the expression for the stator currents of higher harmonics can be written without the value of R_{kh} as:

$$\frac{I_{sh}}{j \cdot X_{khr}} = \frac{U_{sh}}{j \cdot X_{khr}} \quad (4)$$

where: U_{sh} is the RMS value of the supply voltage harmonic h . Approximately, based on the author's experience [4], the saturation of magnetic paths for the leakage fluxes of the machine windings was taken into account, which, however, did not change the form of the expression to I_{sh} – only the short-circuit reactance of the equivalent circuit for the first harmonic X_{klr} was replaced with the same reactance, but saturated X_{klr_nas} (the value derived from the measurement of the input impedance of the machine phase at $s = 1$ and the full rated voltage U_{sN} with the frequency f_N), i.e. lower than the unsaturated value X_{klr} (according to [4] typically by 20%). Finally, the I_{sh} current was written as:

$$\frac{I_{sh}}{j \cdot X_{khr_nas}} = \frac{U_{sh}}{j \cdot X_{klr_nas} \cdot h^{0.8}} \quad (5)$$

With these assumptions, the expression for the relative value of the motor load torque limit was derived as a function of the defined factor *HVF* (*Harmonic Voltage Factor*):

$$\frac{M_{obcdop}}{M_N} = \sqrt{1 - 35 \cdot HVF^2} \quad (6)$$

$$HVF = \sqrt{\sum_{h=5}^{19} \frac{U_{sh_rel}^2}{h}} \quad (7)$$

The expression (7) was written for the rotating harmonics with the highest number $h = 19$ because in [4] it was found that the remaining higher supply frequencies did not affect the motor operation.

The aim of the measurements presented in the paper was to investigate the effect of supplying a cage induction motor with a voltage containing higher harmonics on its thermally limit of load torque, as well as to verify the validity of using the HVF factor and the expression (6) to assess the torque load limit of an induction motor supplied with such voltage.

The measuring system

In order to test the performance of the cage induction motor under distorted voltage supply, a measuring stand was built, as detailed in Figure 1. The stator winding of the motor was star connected and powered from a programmable IT7627 frequency converter (manufactured by ITECH), which was powered from a 400V / 50Hz three-phase grid, enabling the tested motor to be supplied with a distorted, symmetrical, three-phase voltages. The motor was connected to the converter with a shielded four-conductor cable, with the shield connected to the inverter shield. The measurements of currents, voltages, and the electric power of the motor (both the active and reactive power taken from the power source, as well as its apparent power) were carried out with the use of voltage and current converters with Hall sensors. The UW and VW voltages, together with the U and V currents of the power cables of the motor were measured. The voltage and current measurement paths have been calibrated with the use of the CP11B single-phase power calibrator (manufactured by Calmet). The output voltage signals of the voltage and current converters were transferred to the SCB68A connection terminal, which was connected to the PCIe-6340 measurement card (manufactured by National Instruments), mounted in the PCIe slot of the mainboard of a desktop PC via a 68-pin SCSI connector.

The shaft of the tested motor was coupled with the shaft of a separately excited DC machine by two clutches (manufactured by KTR). A DATAFLEX 32/100 torque sensor (manufactured by KTR) was placed between the clutches. The output signals from the torque sensor (the torque signal and the signal of the rotation speed of the shaft) were connected to the DF2 terminal, which was powered by the laboratory power supply DC 24V. The output signals from the DF2 terminal were sent to the terminal SCB68A. In order to provide the ability to smoothly adjust the load of the tested motor, the excitation winding of the DC machine was powered from a single-phase autotransformer, to which a Graetz diode bridge was connected, loaded with a capacitor with the capacity of 470 μ F. The armature of the DC machine was loaded with constant resistance.

All the conductors carrying the measurement signals to the SCB68A terminal and to the measurement card were, in fact, separate, two-wire screened cables, with the screens zeroed on the side of the measuring computer. The measured signals were sampled at a frequency of 10 kHz each.

Three Pt100 temperature sensors were placed in one phase of the stator of the motor (during its assembly by the manufacturer). They were mounted on the front connection of the phase winding on the fan side, on the front connection on the opposite side, and inside one of the stator slots. The lead wires of the Pt100 temperature sensors were connected to the dedicated 6ED1055-IMD00-0BA2 temperature transmitters (manufac-

tured by Siemens), which, in turn, were connected to the PLC LOGO controller (also manufactured by Siemens).

After the assembling of the measuring stand, programs for reading and recording the measurement data in the DASyLab (manufactured by National Instruments) and LOGO environment were written. Thanks to the program for the LOGO controller, it was possible to read the three-point temperature of the phase winding of the motor. The DASyLab environment allowed for the measurement and visualization of the currents, voltages, and rotational speed, as well as the active and reactive power drawn from the power source by the motor, in real-time, with the possibility of saving measured values in files.

The tested induction motor was manufactured by Tamel. Its nameplate is depicted in Figure 2.

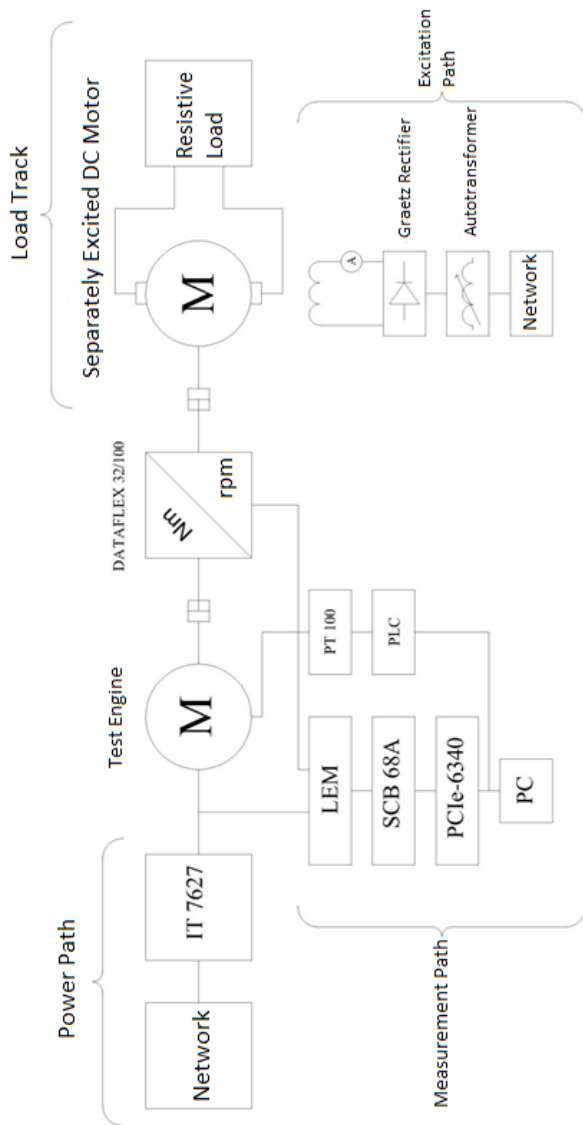


Figure 1. Diagram of the test stand

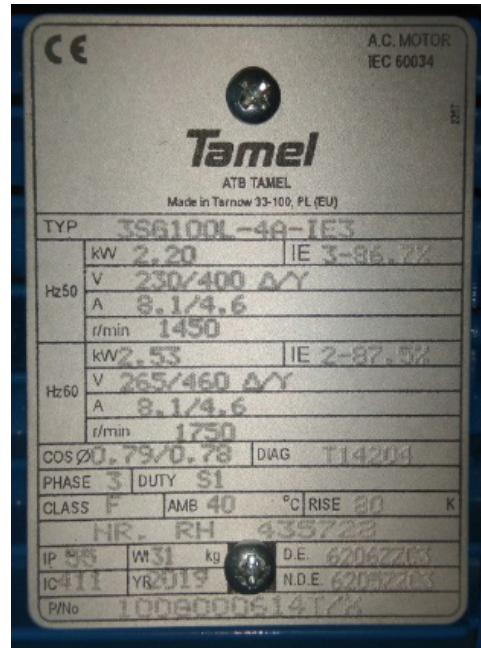


Figure 2. Rated data of the tested motor

The measurement methodology

After the performing of the frequency start-up of the motor with a given power supply, it was loaded with such a torque, that the total active power consumed by the motor was equal to its rated electric active power (from the power source), i.e. 2550W. Then, the values of all three measured temperatures for the phase windings of the motor needed some time to establish themselves. In the meantime, the value of the power of the motor was monitored, and the necessary corrections from the side of the loading machine were being made.

The first series of measurements concerned the status of supplying the motor with rated voltage. Their results became reference results, necessary for interpreting the measurement results of the motor supplied with distorted voltages. The next few series of measurements concerned the motor powered with symmetrical distorted voltage, with the following parameters:

1. with the content of the 5th harmonic with the RMS value amounting for 10% of the RMS value of the fundamental harmonic voltage,
2. with the content of the 5th harmonic with the RMS value amounting for 20% of the RMS value of the fundamental harmonic voltage,
3. with the content of the 7th harmonic with the RMS value amounting for 10% of the RMS value of the fundamental harmonic voltage,
4. with the content of the 7th harmonic with the RMS value amounting for 20% of the RMS value of the fundamental harmonic voltage,
5. with a square wave (many harmonics).

The results of the measurements

Figures 3–8 show the waveforms of the motor phase current in the tested power conditions.

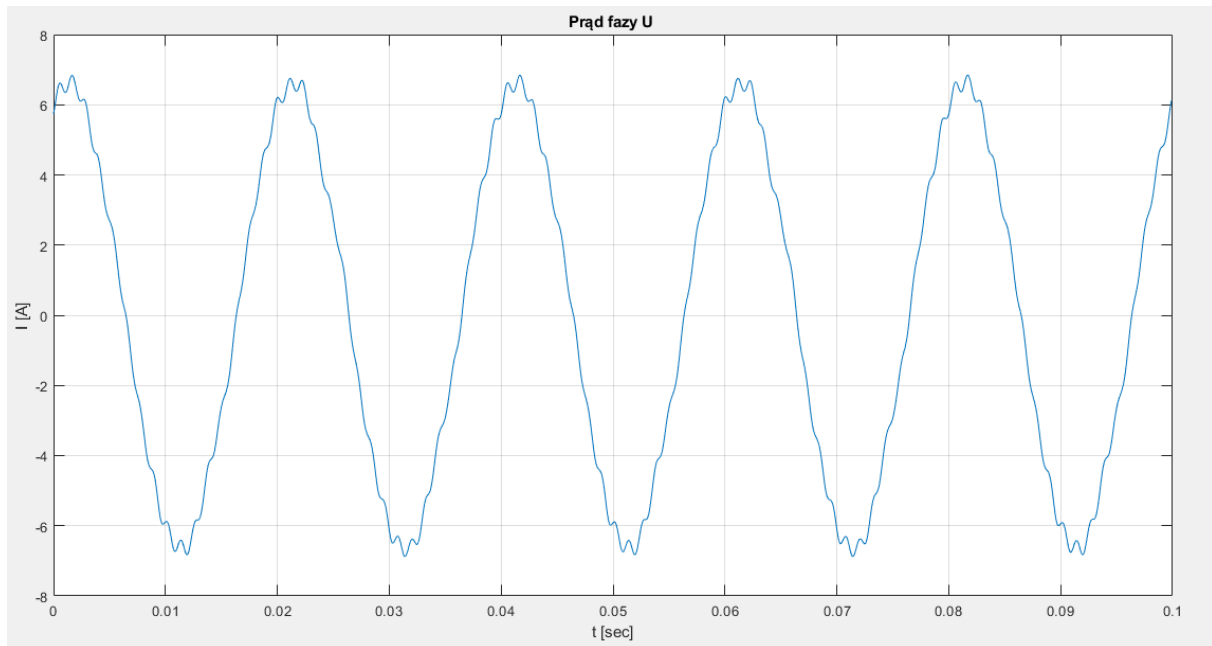


Figure 3. The waveform of the phase current of the motor supplied with rated voltage (sinusoidal voltage). The visible higher harmonics are slot harmonics of the machine current

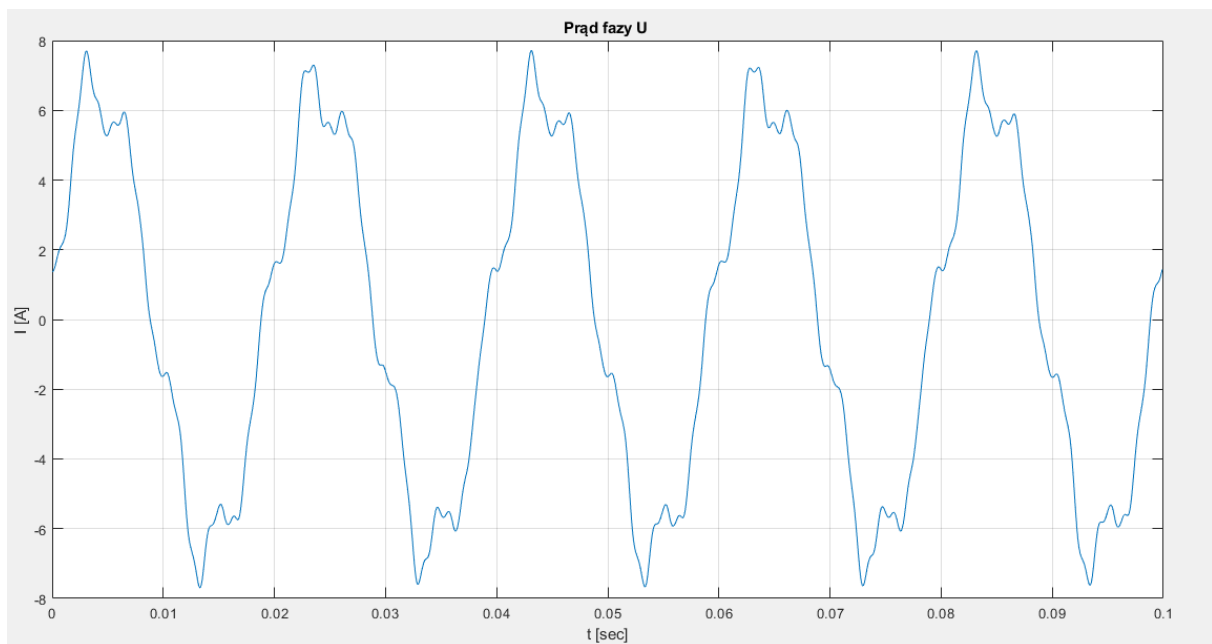


Figure 4. The waveform of the phase current of the motor supplied with a voltage of 10% of the 5th harmonic

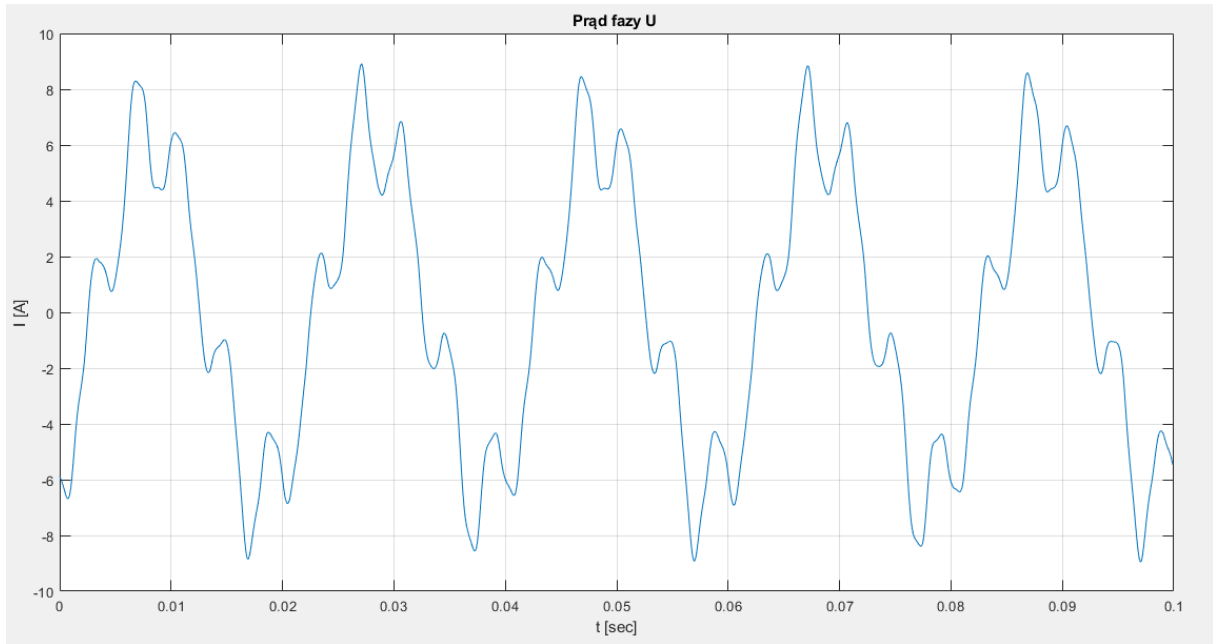


Figure 5. The waveform of the phase current of the motor supplied with a voltage of 20% of the 5th harmonic

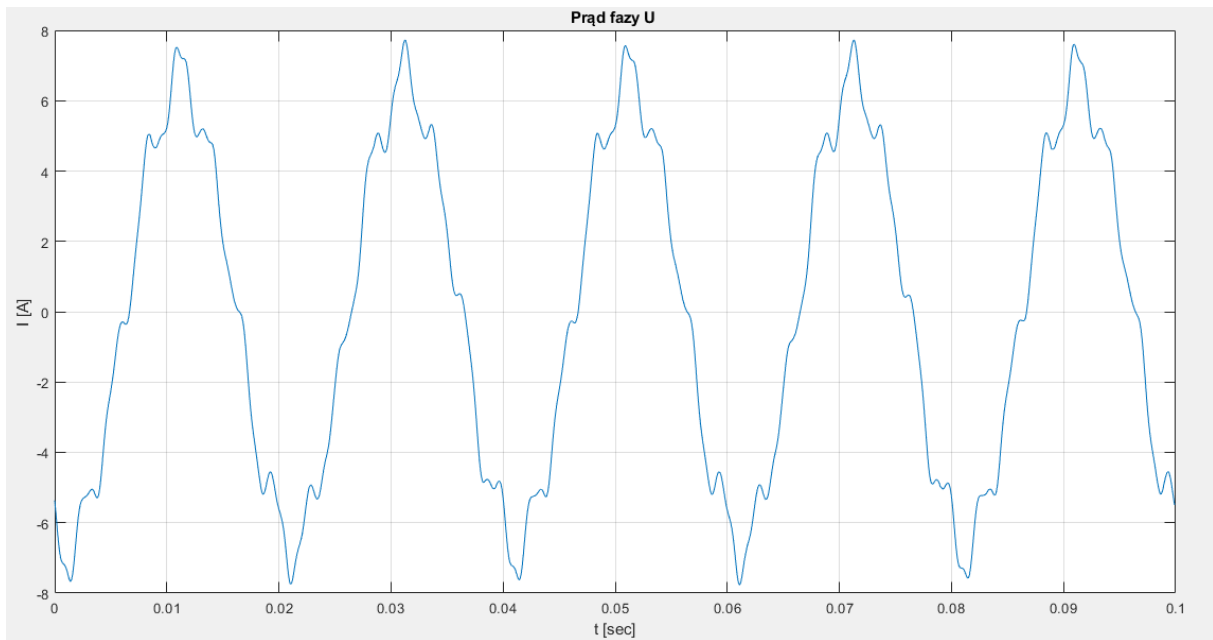


Figure 6. The waveform of the phase current of the motor supplied with a voltage of 10% of the 7th harmonic

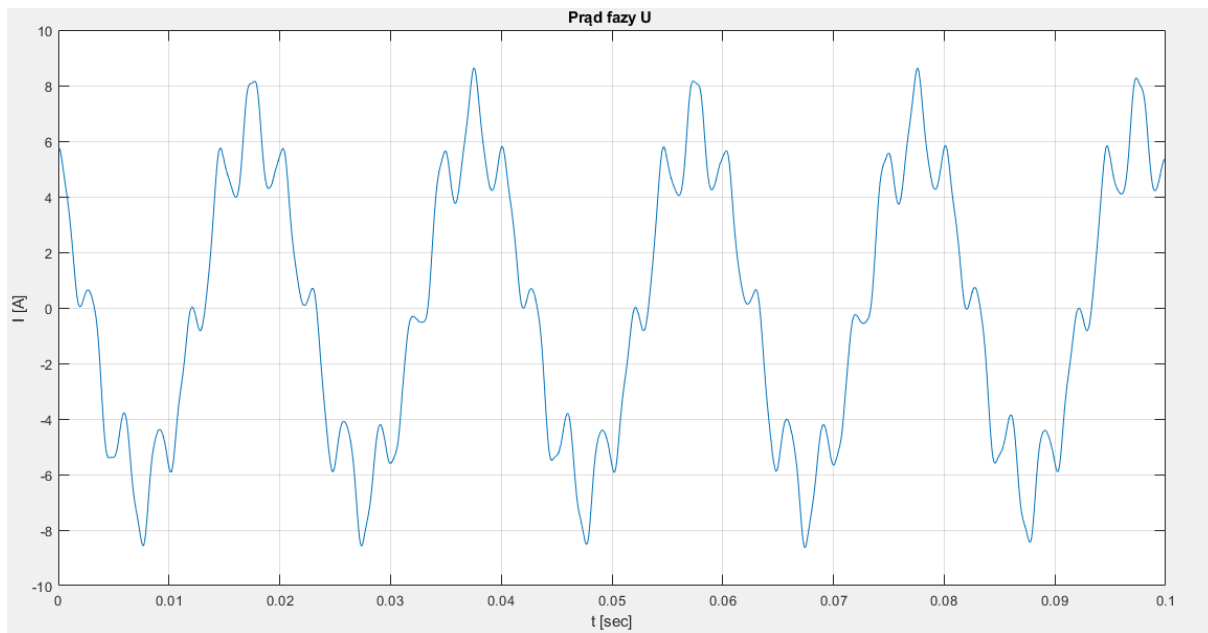


Figure 7. The waveform of the phase current of the motor supplied with a voltage of 20% of the 7th harmonic

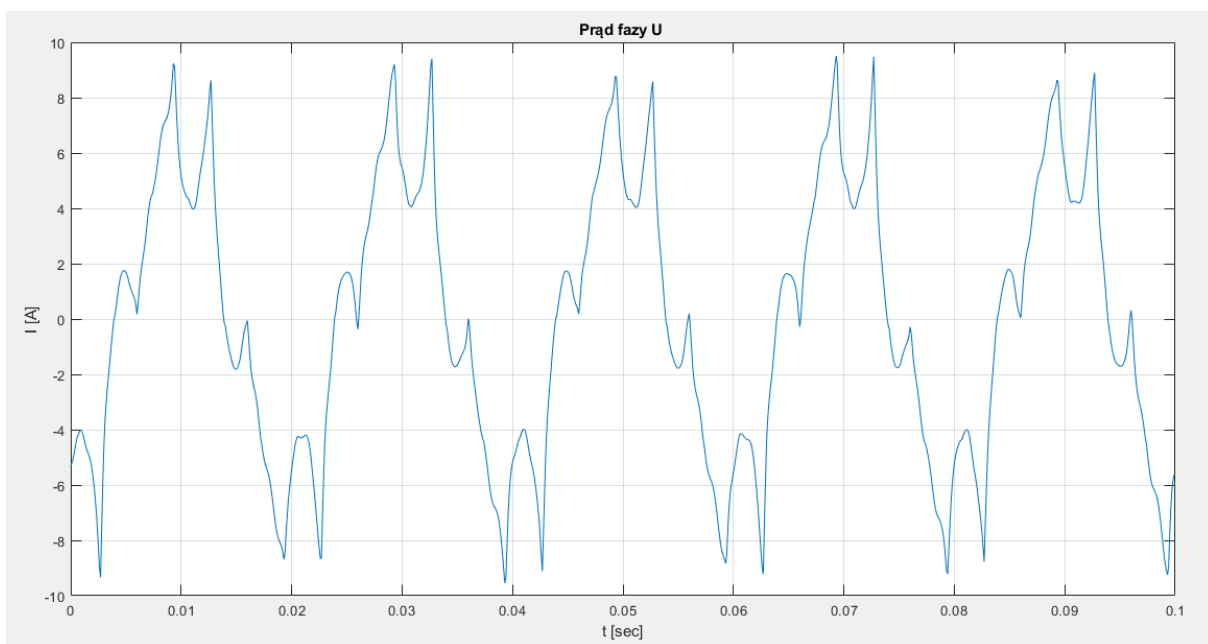


Figure 8. The waveform of the phase current of the motor supplied with rectangular voltage

Table 1 shows the numerical results of the measurements. The THD coefficients of the voltages and currents were calculated as:

$$THD = \frac{\sqrt{\sum_{h=2}^{50} X_h^2}}{X_1} \tag{8}$$

where: X_h is the RMS value of the h harmonic of the line voltage or motor phase current; and X_1 is the RMS value of the basic harmonic ($h = 1$) of the line voltage or motor phase current.

Shown in Table 1 the largest of the three measured temperature increases of the motor phase winding was calculated as:

$$\Delta T = T_U - T_O \tag{9}$$

where: T_U is the maximum temperature of the motor phase; and T_O is the motor ambient temperature.

The thermally permissible motor load torque was calculated according to the mathematical expression:

$$M_{dop} = M_n \frac{\Delta T}{\Delta T_n} \tag{10}$$

where: M_n is the motor rated torque; ΔT_n is the rated temperature rise of the motor phase above the rated ambient temperature of 40°C; ΔT is the temperature increase of the motor phase above the ambient temperature during the measurements.

these torques is approximately 1 N·m, which makes up 7% of the machine rated torque. Such difference is the result of both the presence of higher slot harmonics in the motor currents and the simultaneous presence of many harmonics in the supply voltage.

Table 1. The comparison between the results of the measurements and calculations

Power →	Rated Power	10% of the 5 th harmonic	20% of the 5 th harmonic	10% of the 7 th harmonic	10% of the 7 th harmonic	Square Power
Value ↓						
THD_U	0%	10%	20%	10%	20%	30%
THD_I	2%	16%	33%	12%	24%	35%
U_{sk} [V]	404	401	402	401	402	399
I_{sk} [A]	4.70	4.76	4.90	4.73	4.80	4.96
$P_{consumed}$ [W]	2553	2551	2548	2549	2549	2552
[°C]	19.0	19.3	19.7	18	17	16
[°C]	57.5	60.5	65.0	58	60	62.8
[°C]	38.5	41.2	45.3	40	43	46.8
[N·m]	14.49	13.54	12.31	13.95	12.97	11.92
HVF [-]	0	0.0447	0.0894	0.0378	0.0756	0.1120
[N·m]	14.49	13.97	12.29	14.12	12.96	10.86

The expression (10) was derived with the assumption that both the set rise in the temperature of the motor phase and the mean electromagnetic torque of the motor depend on the square of the RMS value of its current. The HVF value was calculated only up to the 19th harmonic, according to the (7).

Conclusions

The rated current of the tested motor is distorted from the sinusoid, and the higher harmonics visible in its course (Fig. 3) have a frequency corresponding to the number of the stator slots. The THD_I current distortion coefficient is 2%, which is a level acceptable by the literature [7]. Due to the presence of slot harmonics in the machine currents, their THD_I coefficient is always greater than the THD_U of the supply voltage (Table 1). The opposite relationship should be expected on the basis of the induction machine equivalent diagrams for individual rotating harmonics.

The comparison of the calculated permissible load torque values based on the HVF (M_{dopHVF}) and based on the measurements of the maximum winding temperature (M_{dop}) shows that despite many simplifying assumptions accompanying its design, the HVF is a fully useful tool for determining the permissible load capacity of the motor supplied with a voltage containing a limited amount of higher harmonics. When supplying the motor with rectangular voltage (with the highest THD_U and THD_I tested coefficients of 30% and 35% respectively), the difference between

The method of deriving the HVF does not consider the slots of the machine as a source of higher frequencies in the machine currents. It attributes their presence only to the appropriate additional frequencies in the motor supply voltage. It is worth noting that the inclusion of harmonics with numbers higher than 19 in the HVF will result in a further decrease in the motor load torque permissible by the formula (6), and thus an increase in the discrepancy between the torque is calculated from (6) and (10).

Author Contributions

Conceptualization, methodology, validation, formal analysis, writing – original draft preparation, data curation, writing – review and editing, supervision, project administration, funding: Tomasz Drabek. Investigation, resources, acquisition, visualization: Krzysztof Krzyściak.

References

1. Gała M, Jagieła K, Kępiński M, Rak J. Oddziaływanie dużych napędów przekształtnikowych prądu stałego na parametry eksploatacyjne silników asynchronicznych, Zeszyty Problemowe – Maszyny Elektryczne, 2007;76:35-40.
2. de Abreu JPG, and Emanuel AE. Induction Motor Thermal Aging Caused by Voltage Distortion and Imbalance: Loss of Useful Life and Its Estimated Cost, IEEE Transactions

- on Industry Applications, 2002;38(1):12–20.doi: <https://doi.org/10.1109/28.980339>.
3. Frank S, Lee K, Sen PK, Polese LG, Alahmad M, Waters C. Reevaluation of Induction Motor Loss Models for Conventional and Harmonic Power Flow, Proceedings of the 2012 North American Power Symposium (NAPS), 2012 Sep9-11; Champaign, IL, USA. IEEE; 2012.doi: <https://doi.org/10.1109/NAPS.2012.6336382>.
 4. Cummings PG. Estimating Effect of System Harmonics on Losses and Temperature Rise of Squirrel-Cage Motors, IEEE Transactions on Industry Applications, 1986;IA-22 (6):1121-1126.doi: <https://doi.org/10.1109/TIA.1986.4504843>.
 5. Drabek T. Praca silnika indukcyjnego zasilonego napięciem zawierającym subharmoniczne, Science, Technology and Innovation, 2017;1(1):27-34.doi: <https://doi.org/10.5604/01.3001.0010.7665>.
 6. Drabek T. Praca silnika indukcyjnego zasilonego napięciem zawierającym interharmoniczne, Science, Technology and Innovation, 2018;1(2):47-53.doi: <https://doi.org/10.5604/01.3001.0012.1305>.
 7. Hanzelka Z. Jakość dostawy energii elektrycznej, Kraków: Wydawnictwa AGH; 2013.